Article

Discovery Medicine 2026; 38(212): 2975–2989
https://doi.org/10.24976/Discov.Med.202638212.229

Knockdown of CHI3L1 Attenuates Venous Intimal Hyperplasia by Modulating Vascular Inflammation and Oxidative Stress via the JNK/ERK Pathway

Sishi Yan[1], Ji Xu[1], Fengliang Yao[1], Xuebo Chen[1,*]

[1]Department of Nephrology, Zhoushan Hospital, Wenzhou Medical University, 316021 Zhoushan, Zhejiang, China
*Correspondence: zscxb01@163.com (Xuebo Chen)
Submitted: 5 March 2026 Revised: 30 April 2026 Accepted: 25 May 2026 Published: 23 September 2026

Background: Venous intimal hyperplasia (VIH) is the key pathological basis for early failure of arteriovenous fistula (AVF) and for stenosis of hemodialysis access. Chitinase-3-like protein 1 (CHI3L1) is highly expressed during cardiovascular remodeling and inflammation, but its role and underlying mechanisms in AVF-related VIH remain unclear.

Methods: A rat AVF model was established, and VIH, inflammatory cell infiltration, and changes in the CHI3L1/c-Jun N-terminal kinase (JNK)/extracellular signal-regulated kinase (ERK) pathway were assessed at 7 and 21 days after surgery. Adenovirus-mediated CHI3L1 knockdown was used to evaluate its effects on VIH, oxidative stress, and inflammation. *In vitro*, a human vascular smooth muscle cell (VSMC) activation model was induced by platelet-derived growth factor-BB (PDGF-BB), and a stable CHI3L1-knockdown cell line was generated. VSMC proliferation, migration, phenotypic switch, oxidative stress, and inflammatory levels were evaluated, and the involvement of JNK/ERK signaling was investigated using the JNK agonist anisomycin.

Results: *In vivo*, venous fistula tissue from the AVF model exhibited a significant increase in CHI3L1 expression, along with neointimal hyperplasia (NIH) and the presence of $CD68^+$ macrophage infiltration ($p < 0.001$). CHI3L1 knockdown reduced JNK/ERK activation, attenuated neointimal thickening, macrophage infiltration, oxidative stress, and inflammatory responses, alongside a reversal in the downregulation of contractile marker proteins ($p < 0.001$). *In vitro*, PDGF-BB induced upregulation of CHI3L1 in VSMCs ($p < 0.001$). CHI3L1 knockdown suppressed VSMC proliferation, migration and the contractile-to-synthetic phenotypic switch, reduced inflammatory cytokine secretion and oxidative stress markers, and inhibited JNK/ERK phosphorylation ($p < 0.001$); these effects were partially reversed by anisomycin.

Conclusion: CHI3L1 knockdown significantly inhibits activation of the JNK/ERK signaling pathway, mitigates vascular wall inflammation and oxidative stress, thereby blocking pathological phenotypic transformation, excessive proliferation, and migration of VSMCs, ultimately attenuating AVF-related VIH.

Keywords: CHI3L1; oxidative stress; inflammation; venous intimal hyperplasia; endothelial cells

Introduction

Venous intimal hyperplasia (VIH) is the central pathological basis for arteriovenous fistula (AVF) failure and hemodynamic impairment, and represents one of the most common and challenging problems in hemodialysis for end-stage renal disease patients [1]. Despite being regarded as the optimal dialysis access due to its advantages in long-term patency and lower infection risk, the AVF still faces challenges in maintaining satisfactory long-term patency. A substantial proportion of AVF failure is attributed to intimal hyperplasia (IH)–induced vascular stenosis, reduced blood flow, and even occlusion [2,3]. VIH development entails a complex interplay of pathological processes, such as vascular smooth muscle cell (VSMC) proliferation/migration, inflammation, oxidative stress, and extracellular matrix (ECM) deposition [4], among which phenotypic switching and excessive proliferation of VSMC are considered pivotal events [5]. However, VSMC phenotypic switching and excessive proliferation do not occur in isolation; their initiation and progression are jointly regulated by various microenvironmental factors. Among the numerous factors influencing vascular remodeling, inflammation and oxidative stress are regarded as key drivers of IH onset and progression [6,7]. Vascular injury prompts significant inflammatory cell infiltration and mediator release. This process directly activates VSMCs to proliferate and migrate, which contributes to accelerated intimal remodeling [8]. Moreover, oxidative stress—triggered by an overproduction of reactive oxygen species (ROS) from both hemodynamic alterations and cellular damage—further exacerbates the condition by activating pathways related to inflammation and cell injury, which in turn progressively compromise vascular wall structure [9]. Inflammation and

oxidative stress mutually reinforce each other and collectively promote the development of vascular stenosis [10]. Therefore, elucidating the key molecules that regulate these two processes may help identify new strategies to halt VIH.

Chitinase-3-like protein 1 (CHI3L1) is a glycoprotein structurally similar to chitinases that is widely involved in inflammation, tissue remodeling, cell migration, and fibrosis, among other biological processes [11,12]. Elevated expression of CHI3L1 has been observed in various vascular pathologies, such as atherosclerosis, diabetic vascular complications, and vascular injury repair, indicating its potential significance in vascular remodeling [13,14,15]. CHI3L1 can promote VSMC proliferation and migration and enhance local inflammatory responses by activating inflammation-related signaling pathways [16]. Moreover, increased CHI3L1 expression has been reported to correlate closely with failure of autologous AVF in patients with end-stage renal disease [17], implying that CHI3L1 may participate in the development of VIH and stenosis; however, its precise mechanisms of action remain unclear. In particular, whether CHI3L1 contributes to this process by regulating oxidative stress, and whether it involves key intracellular signaling pathways, remains to be demonstrated experimentally. Therefore, further in-depth investigation of CHI3L1 in AVF-induced VIH—especially regarding its relationship with inflammatory responses, oxidative stress, and the related signaling pathways—will help clarify the pathological mechanisms underlying AVF dysfunction and provide a theoretical basis for developing novel therapeutic strategies.

Among the signaling pathways that regulate vascular cell behavior, c-Jun N-terminal kinase (JNK) and extracellular signal-regulated kinase (ERK), two major members of the mitogen-activated protein kinase (MAPK) family, have been extensively shown to play central roles in inflammation, oxidative stress, proliferation, and migration [18,19,20]. Activation of JNK and ERK signaling is often triggered by stimuli such as growth factors, cytokines, and oxidative stress, thereby promoting phenotypic switching and proliferation of VSMCs [21,22]. Platelet-derived growth factor-BB (PDGF-BB), a prototypical VSMC activator, can induce cell proliferation and migration and is a classical tool for modeling the IH microenvironment [23]. CHI3L1 has been implicated in the modulation of MAPK pathway activity based on earlier findings [24], but the specific regulatory relationships, whether it influences vascular inflammation and oxidative stress through this pathway, and the relevance of this mechanism to VIH have not been clearly established. On this basis, the present study established an AVF animal model and a PDGF-BB–induced VSMC model to systematically evaluate the effects of CHI3L1 knockdown on VIH. At the same time, by assessing inflammatory cytokine levels, oxidative stress markers, and the JNK/ERK pathway, we explored the molecular mechanisms by which CHI3L1 participates in vascular remodeling. This research aims at clarifying the pivotal function of CHI3L1 in VIH development and at determining its regulatory influence on inflammation and oxidative stress through JNK/ERK signaling. The ultimate goal is to identify new molecular avenues for preventing and treating AVF failure.

Materials and Methods

Establishment of the Rat AVF Model

Sixty-three male Sprague–Dawley rats (350–450 g, 12–16 weeks old) were purchased from Jiangxi Laib Biotechnology Co., Ltd. (Nanchang, China). All rats were housed under controlled environmental conditions (temperature 22 ± 2 °C, relative humidity 50% ± 5%) with a 12 h light/12 h dark cycle, and had free access to water and standard chow. All animal experiments were approved by the Zhejiang Free Trade Zone Ruisai Biopharmaceutical Technology Limited Company Experimental Animal Welfare and Ethics Committee Ethics Committee (Approval Number: 2024073179). A total of 36 rats were used, with 18 rats in each group. They were randomly divided into the control group and the AVF model group.

Rats were anesthetized via an intraperitoneal injection of ketamine/xylazine/atropine cocktail (100/10/0.05 mg/kg) and then secured in a supine position. Following shaving and disinfection of the right groin, a longitudinal incision was performed superior to the inguinal ligament to reveal the common femoral artery (CFA), femoral vein, and superficial epigastric vein (SEV). A microvascular clamp was applied to temporarily occlude blood flow in the CFA and SEV, and the vascular lumen was flushed with a rinsing solution (final concentration approximately 50 IU/ml heparin in 0.9% sodium chloride). The distal SEV was transected to create a venous end, and a small side window was made in the CFA to serve as the arterial opening. The AVF was then created by anastomosing the SEV end to the CFA side window using 10-0 monofilament nylon microsutures [25]. After completion of the anastomosis, the venous clamp was released first, followed by the arterial clamp. The anastomotic site was inspected for bleeding and gently compressed to achieve hemostasis. Successful AVF creation was confirmed by rapid filling and dilation of the SEV, a change in color from dark red to bright red, visible pulsation or palpable thrill, and absence of active bleeding or thrombus formation [26]. The wound was then irrigated, followed by layered closure of the muscle and subcutaneous tissue, followed by continuous skin closure with 10-0 nylon sutures.

In the control animals, having undergone the same anesthetic and surgical exposure procedures, only the CFA and related veins were exposed and dissected free without vascular incision or anastomosis, followed by routine hemostasis and wound closure. Postoperatively, rats were monitored daily for general condition, body weight

changes, and wound healing. Animals were deeply anesthetized with an intraperitoneal injection of sodium pentobarbital (150 mg/kg) and then euthanized by cervical dislocation at the predetermined endpoints of 7 and 21 days post-surgery. Under a microscope, the vessels were carefully dissected along the AVF tract; a 0–6 mm segment of the venous limb proximal to the arteriovenous anastomosis was harvested as AVF venous tissue for the AVF group, while the femoral vein at the corresponding anatomical location was collected as control venous tissue in the control group.

Establishment of the Rat CHI3L1 Knockdown Model

The rats were randomly divided into the sham operation group, the injured + shNC group, and the injured + shCHI3L1 group, with 9 rats in each group, totaling 27 rats. Rat CHI3L1 shRNA (shCHI3L1 sequence, 5′-CACTGAGAGACGCACTGCTTTTTCAAGAGAAAAGCAGTGCGTCTCTCAGTGTTTTT-3′) and shNC (5′-TTCTCCGAACGTGTCACGTTTCAAGAGAACGTGACACGTTCGGAGAATTTTT-3′) were synthesized and packaged into adenoviruses by RiboBio Co., Ltd. (Guangzhou, China). Immediately after completion of the AVF procedure, adenoviral suspension (5×10^8 PFU) was locally injected into the venous wall tissue surrounding the anastomotic site and maintained *in situ* for 30 min [27]. The sham-operated group received an equal volume of normal saline. At 21 d postoperatively, rats were euthanized by cervical dislocation, serum was collected, and venous tissue at the anastomotic site (including the IH region) was isolated for subsequent analyses.

Histopathological Examination

Hematoxylin and Eosin (HE) Staining

The harvested rat venous vascular tissues were subjected to 24 h fixation in 4% PFA (G1101, Servicebio, Wuhan, China); subsequently, they were dehydrated, embedded in paraffin, and cut into 4 μm-thick sections. Following deparaffinization and rehydration, sections were processed for H&E staining with hematoxylin (G1004, Servicebio; 5 min) and eosin (G1001, Servicebio; 3 min). Images were acquired using a light microscope (BX53, Olympus, Tokyo, Japan), and the intimal and medial areas were manually delineated and measured using ImageJ software (version 1.53, National Institutes of Health, Bethesda, MD, USA). The IH severity ratio was defined as the intima-to-media area ratio (Neointimal/Media ratio). The intimal area was defined as the region between the luminal endothelium and the internal elastic lamina, and the medial area was defined as the region between the internal elastic lamina and the external elastic lamina.

Immunohistochemistry (IHC)

After deparaffinization, rehydration, and antigen retrieval (citrate buffer, ZLI-9065, ZSGB-BIO, Beijing, China), sections were treated to block endogenous peroxidase (3% H_2O_2) and non-specific binding (10% goat serum, 164212, Procell, Wuhan, China). They were incubated with primary antibodies (CD68: 1:500, 83014-5-RR, Proteintech, Wuhan, China; Ki67: 1:600, AN004340L, Elabscience, Wuhan, China) overnight at 4 °C, followed by secondary antibodies (1:1000, E-AB-1003, Elabscience) for 1 h at room temperature. Staining was visualized with DAB (E-IR-R101, Elabscience) and counterstained with hematoxylin. Stained sections were imaged under a microscope. The number of CD68-positive cells and the percentage of Ki67-positive cells were quantified.

Cell Culture

VSMCs (CRL-1999) were obtained from ATCC (Manassas, VA, USA) and cultured in DMEM (11885084, Gibco, Grand Island, NY, USA) supplemented with 10% FBS (PM00011, Proteintech) in a humidified incubator at 37 °C with 5% CO_2 [28]. To guarantee optimal viability and a stable phenotype, subsequent experiments were conducted using cells harvested during the logarithmic growth phase between passages 3 and 5. The VSMC cell line was authenticated by STR profiling and tested negative for mycoplasma contamination.

Cell Treatment

CHI3L1 Knockdown

To target the human *CHI3L1* gene, we designed and synthesized a specific short hairpin RNA (shRNA) sequence, shCHI3L1 (5′-CAAGGAAATGAAGGCCGAATT-3′), and a negative control shNC (5′-TTCTCCGAACGTGTCACGT-3′). The shRNA sequences were cloned to create lentiviral plasmids pLV-shCHI3L1 and pLV-shNC, with viral packaging and titration performed by RiboBio. VSMCs were then transfected with these plasmids using PEI (GF40062675, Sigma, St. Louis, MO, USA) at 60–70% confluence. A stable knockdown line was established through puromycin selection (2 μg/mL; ST551, Beyotime, Shanghai, China), and knockdown efficacy was verified via Western blot.

Cell Viability Assay

The experimental concentrations of PDGF-BB and anisomycin were determined by assessing VSMC viability. Cell viability was assessed by CCK-8 assay following treatment. Cells (5×10^3/well, triplicate) in 96-well plates were treated with PDGF-BB (0-160 ng/mL, 24 h; GF149, Sigma) or anisomycin (0–160 ng/mL, 1 h; a JNK agonist, HY-18982, MCE, Monmouth Junction, NJ, USA). After adding 10 μL of CCK-8 reagent (ANT181M, AntGene, Wuhan, China) to each well and incubate at 37 °C for 3 h. Subsequently, measure the OD values at a wavelength of 450 nm using a microplate reader (Synergy H1, BioTek, Winooski, VT, USA) to assess cell viability.

Cell Grouping and Drug Treatment

To assess the impact of CHI3L1 knockdown on VSMC proliferation and migration, cells were allocated to four treatment groups: (1) con+NC: VSMCs cultured in normal medium and transfected with shNC; (2) con+shCHI3L1: cells transfected with shCHI3L1 and maintained in normal medium; (3) PDGF-BB+shNC: VSMCs transfected with shNC followed by stimulation with 20 ng/mL PDGF-BB for 24 h; (4) PDGF-BB+shCHI3L1: VSMCs transfected with shCHI3L1 followed by stimulation with 20 ng/mL PDGF-BB for 24 h. Cell proliferation and migration were assessed using CCK-8, EdU staining, and Transwell assays.

To further investigate the JNK/ERK pathway in the above process, VSMCs were divided into four groups: (1) control: standard conditions; (2) PDGF-BB+shNC: VSMCs transfected with shNC and then stimulated with PDGF-BB; (3) PDGF-BB+shCHI3L1: VSMCs transfected with shCHI3L1 and then stimulated with PDGF-BB; (4) PDGF-BB+shCHI3L1+Anisomycin: VSMCs transfected with shCHI3L1 were pretreated with 20 ng/mL Anisomycin for 1 h before PDGF-BB stimulation, followed by PDGF-BB induction for 24 h.

Transwell Assay

A Transwell-based migration assay was conducted to quantify cell migration and to screen for the optimal stimulating concentration of PDGF-BB. After 24 h PDGF-BB pretreatment, cells (5×10^4/well) were seeded in serum-free medium (22600050, Gibco) into the upper chambers of Transwell inserts (8 µm, Corning). The lower chambers were loaded with 600 µL of medium supplemented with 10% FBS. Following 24 h of incubation, cells remaining on the upper surface were wiped off. Migrated cells on the lower surface were fixed with 4% PFA (15 min), stained with crystal violet solution (0.1%, 60505ES25, Yeasen, Shanghai, China; 20 min), and manually counted in five randomly chosen microscopic (BX53, Olympus) fields to assess migratory capacity.

Flow Cytometry

CHI3L1 expression and ROS levels were analyzed in separate cell samples. For flow cytometric analysis of CHI3L1, cells were stained intracellularly using anti-CHI3L1 antibody (1:100, MA5-36122, Invitrogen) and an Alexa Fluor 488-conjugated secondary (1:500, A-10680, Invitrogen), with unstained controls. Fluorescence was measured to determine expression levels. Cells were stained with DCFH-DA (10 µM, S0033, Beyotime) at 37 °C for 30 min (dark). Flow cytometry (BD FACSCanto II flow cytometer, BD Biosciences, San Jose, CA, USA) was then used to detect DCF fluorescence (488/525 nm), with intensity corresponding to intracellular ROS levels.

EdU Assay

Cell proliferation was evaluated using an EdU assay kit (C0078L, Beyotime). After treatment, cells on coverslips were EdU-pulsed for 2 h, then fixed, permeabilized, and stained via click chemistry and DAPI. The percentage of EdU+ nuclei was calculated from fluorescence micrographs (IX73, Olympus) to determine proliferation rates.

Biochemical Assays

Rat venous vascular tissues were collected, weighed, and homogenized in pre-chilled PBS at a tissue mass-to-PBS volume ratio of 1:9, followed by centrifugation to obtain the supernatant for subsequent use. VSMCs from each group were collected, lysed, and centrifuged, and the supernatant was collected. The levels of SOD (BC5165, Solarbio, Beijing, China), MDA (BC0020, Solarbio), GSH-Px (BC1195, Solarbio), and NAD(P)H (BC0510, Solarbio) were measured using the corresponding assay kits. Samples were added to the working solutions according to the manufacturers' instructions, and absorbance was measured at 450/532/412/340 nm using a microplate reader (Synergy H1, BioTek).

Enzyme-Linked Immunosorbent Assay (ELISA)

Rat-specific ELISA kits were used to determine the serum levels of TNF-α (MBS9424865, MyBioSource, San Diego, CA, USA), IL-6 (MBS2515034), and IL-1β (MBS355368) in each group of rats. The culture supernatants of VSMCs from each group were collected after treatment. Human-specific ELISA kits were used to measure the levels of TNF-α (MBS396296), IL-6 (MBS490361), IL-1β (MBS490348), Intercellular Adhesion Molecule 1 (ICAM-1, MBS9135745), and Monocyte Chemoattractant Protein 1 (MCP-1, MBS335458) in the cell supernatants. All procedures were performed strictly in accordance with the manufacturers' protocols. Absorbance was read at 450 nm using a microplate reader (Synergy H1, BioTek), and the concentrations of the corresponding proteins were calculated from standard curves.

Immunofluorescence (IF)

For IF, dewaxed sections underwent antigen retrieval, permeabilization (0.1% Triton X-100, 10 min), and blocking (BSA, ST023, Beyotime, 1 h). They were then incubated with primary antibodies (α-SMA: 1:400, 67735-1-Ig, Proteintech; CHI3L1: 1:100, PA5-95897, Invitrogen) overnight at 4 °C, followed by fluorescent secondary antibodies (1:500, SA00013-2; 1:200, SA00013-3, Proteintech) for 1 h in the dark. After DAPI nuclear staining (3 min), slides were mounted with anti-fade medium (P0126, Beyotime).

VSMCs were fixed, permeabilized, and blocked, then stained with primary antibodies (α-SMA: 1:1000, 14395-1-AP, Proteintech; Osteopontin (OPN): 1:400, 22952-1-

AP, Proteintech) overnight at 4 °C, followed by fluorescent secondary antibody (1:200, SA00013-2, Proteintech) and DAPI. Images were captured by confocal microscopy (TCS SP8, Leica, Wetzlar, Germany).

Western Blot

Total protein was extracted, quantified, and subjected to SDS-PAGE and Western blotting according to standard protocols. Briefly, after blocking, membranes were incubated with primary antibodies overnight at 4 °C, followed by incubation with HRP-conjugated secondary antibodies (1:5000, SA00001-2, Proteintech). Using chemiluminescent substrate (ECL, PK10001, Proteintech) for visualization, images were acquired using a ChemiDoc MP imaging system (Bio-Rad, Hercules, CA, USA). Software such as ImageJ was used to perform densitometric analysis of the bands and calculate the relative expression levels of the target protein to the internal reference (GAPDH).

The primary antibodies were as follows: CHI3L1 (1:500, PJJ759646, Abmart, Shanghai, China), JNK (1:5000, 51153-1-AP, Proteintech), p-JNK (1:2000, 80024-1-RR, Proteintech), ERK (1:3000, 11257-1-AP, Proteintech), p-ERK (1:1000, 44-680G, Invitrogen), calponin 1 (CNN1; 1:10,000, 13938-1-AP, Proteintech), α-SMA (1:5000, 14395-1-AP, Proteintech), smooth muscle protein 22α (SM22α; 1:10,000, 83922-2-RR, Proteintech), OPN (1:2000, 22952-1-AP, Proteintech), proliferating cell nuclear antigen (PCNA; 1:5000, 10205-2-AP, Proteintech), iNOS (1:5000, 18985-1-AP, Proteintech), NADPH oxidase 2 (NOX2; 1:4000, 19013-1-AP, Proteintech), NADPH Oxidase 4 (NOX4, 1:4000, 14347-1-AP, Proteintech), ICAM-1 (1:10,000, 10831-1-AP, Proteintech), MCP-1 (1:1000, 29547-1-AP, Proteintech), and GAPDH (1:10,000, 10494-1-AP, Proteintech).

Statistical Analysis

All experimental data are presented as mean ± standard deviation (Mean ± SD). Prior to parametric testing, data were subjected to normality testing (Shapiro–Wilk test) and homogeneity of variance testing. Statistical analyses were performed using SPSS 26.0 software (IBM Corp., Armonk, NY, USA). Student's *t*-test was used for comparisons between two groups, while one-way analysis of variance followed by Bonferroni post hoc test was applied for multiple-group comparisons. A p value < 0.05 was considered statistically significant.

Results

Upregulated Expression of CHI3L1 in AVF Venous Lesions in Rats

An AVF rat model was established to mimic the pathological remodeling process of clinical hemodialysis access, with postoperative days 7 and 21 set as key observation time points. HE staining showed that in the AVF group, intimal thickening at the venous side of the anastomosis accompanied by massive cellular accumulation was already evident at day 7. By day 21, a markedly thickened neointima protruded into the lumen, leading to aggravated luminal stenosis, with a clear boundary between the neointima and the media (Fig. 1A). In the AVF group, both the neointimal area (Fig. 1B; $p < 0.001$) and the neointima-to-media ratio (Fig. 1C; $p < 0.001$) of the venous segment were significantly increased at days 7 and 21. CD68 is a transmembrane glycoprotein expressed by the mononuclear–macrophage system and is widely used as a classical marker of macrophage infiltration [29]. IHC results revealed abundant infiltration of CD68-positive cells in AVF venous lesions at days 7 and 21 (Fig. 1D,E; $p < 0.001$), indicating a persistent inflammatory response during venous neointimal hyperplasia (NIH). IF co-localization analysis demonstrated that the proportions of α-SMA$^+$ cells and CHI3L1$^+$ cells were markedly increased in AVF venous lesions at days 7 and 21 (Fig. 1F–H; $p < 0.001$). Furthermore, CHI3L1 protein expression was significantly upregulated in venous lesions of the AVF model (Fig. 1I,J; $p < 0.001$). These findings suggest that CHI3L1 expression in AVF venous lesions in rats is associated with NIH and inflammatory responses.

CHI3L1 Knockdown Inhibits PDGF-BB–Induced VSMC Proliferation, Migration, and Dedifferentiation

NIH is mainly driven by aberrant activation of VSMCs [30]. To further determine whether CHI3L1 directly participates in the regulation of VSMC function, we first established an *in vitro* activation model in human VSMCs induced by PDGF-BB. PDGF-BB at concentrations of 10, 20, and 40 ng/mL increased VSMC viability (Fig. 2A; $p_{10\ ng/mL} = 0.03$, $p_{20\ ng/mL} < 0.001$, $p_{40\ ng/mL} = 0.002$) and promoted their migration (Fig. 2B,C; $p < 0.001$). During PDGF-BB–induced VSMC activation, CHI3L1 protein expression was upregulated (Fig. 2D–G; $p < 0.001$), with the most pronounced increase observed at 20 ng/mL PDGF-BB. Western blot analysis further confirmed that 20 ng/mL PDGF-BB increased CHI3L1 protein expression in a time-dependent manner (0, 6, 12, 24 h) (Fig. 2H,I; $p < 0.001$). All subsequent experiments were conducted under the condition of 20 ng/mL PDGF-BB stimulation for 24 h.

To elucidate the function of CHI3L1, we generated a VSMC cell line with stable CHI3L1 knockdown (shCHI3L1). Western blot analysis verified that shCHI3L1 effectively reduced CHI3L1 protein levels under both basal conditions and PDGF-BB stimulation (Fig. 2J,K; $p < 0.001$). Functional assays showed that CHI3L1 knockdown suppressed VSMC proliferation (Fig. 2L–N; Con: $p_{CCK\text{-}8} = 0.002$, $p_{EdU} = 0.004$; PDGF-BB: $p < 0.001$), and markedly attenuated their migratory capacity (Fig. 2O,P; $p < 0.001$). PDGF-BB stimulation markedly enhanced VSMC proliferation and migration, whereas CHI3L1 knockdown effectively inhibited PDGF-BB–induced cell proliferation and

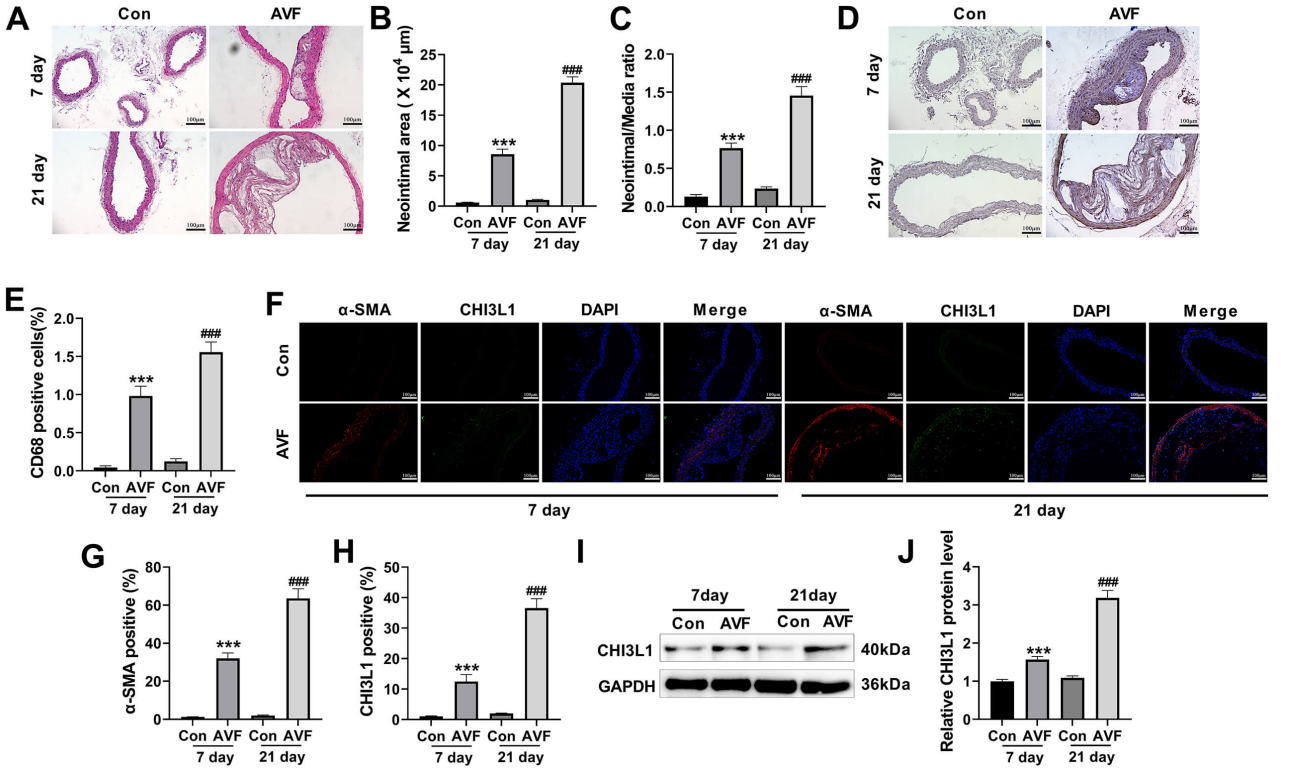

Fig. 1. Upregulated expression of CHI3L1 in AVF venous lesions in rats. (A–C) HE staining images of rat AVF venous lesions (20×, 100 μm). The dashed line delineates the boundary between the neointima and the media. Quantitative analysis of neointimal area and the intima-to-media ratio of AVF veins (7 d, 21 d). (D,E) Immunohistochemical staining of CD68 in AVF venous lesions (7 d, 21 d) (20×, 100 μm). (F–H) IF staining of α-SMA, CHI3L1, and nuclear DAPI in AVF venous lesions showing co-localized expression (7 d, 21 d) (20×, 100 μm). (I,J) CHI3L1 protein expression in AVF venous lesions (7 d, 21 d). n = 9 biological replicates *in vivo* per group. *** $p <$ 0.001 vs Control$_{7\,d}$; ### $p < 0.001$ vs Control$_{21\,d}$. CHI3L1, Chitinase-3-like protein 1; AVF, arteriovenous fistula; HE, Hematoxylin and Eosin; IF, Immunofluorescence; α-SMA, α-smooth muscle actin; DAPI, 4',6-diamidino-2-phenylindole.

migration ($p < 0.001$). PDGF-BB stimulation downregulated the expression of CNN1, α-SMA, and SM22α [31], while significantly upregulating OPN and PCNA expression (Fig. 2Q,R; $p < 0.001$). CHI3L1 knockdown partially reversed these changes ($p < 0.001$). These results indicate that CHI3L1 is a key regulator that mediates PDGF-BB–driven VSMC phenotypic switching toward a dedifferentiated, synthetic phenotype and enhances their proliferative and migratory capacities.

Knockdown of CHI3L1 Reduces PDGF-BB–Induced Oxidative Stress in VSMCs

Oxidative stress is one of the key drivers of pathological activation of VSMCs [32]. To investigate whether CHI3L1 participates in regulating this process, we examined oxidative stress levels and related indicators in VSMCs following PDGF-BB stimulation. The results showed that intracellular ROS levels were significantly elevated in VSMCs treated with PDGF-BB (Fig. 3A,B; $p < 0.001$). PDGF-BB stimulation also reduced the cellular antioxidant capacity, as evidenced by decreased SOD activity (Fig. 3C; $p < 0.001$); the level of MDA, a marker of oxidative damage, was markedly increased (Fig. 3D; $p < 0.001$), whereas the level of NAD(P)H, which reflects cellular reducing capacity, was reduced (Fig. 3E; $p < 0.001$). These findings indicate that PDGF-BB disrupts intracellular redox homeostasis. Knockdown of CHI3L1 markedly ameliorated these changes, suggesting that CHI3L1 may be involved in PDGF-BB–mediated oxidative stress responses. Western blot analysis further showed that PDGF-BB stimulation upregulated the protein expression of iNOS, NOX2, and NOX4 (Fig. 3F,G; $p < 0.001$); after CHI3L1 knockdown, the PDGF-BB–induced upregulation of these pro-oxidant proteins was attenuated ($p < 0.001$). In addition, compared with the con+shNC group, the con+shCHI3L1 group exhibited reduced levels of ROS and MDA, as well as decreased protein expression of iNOS, NOX2, and NOX4. Collectively, these results suggest that CHI3L1 may be an important regulatory factor in PDGF-BB–induced oxidative stress in VSMCs.

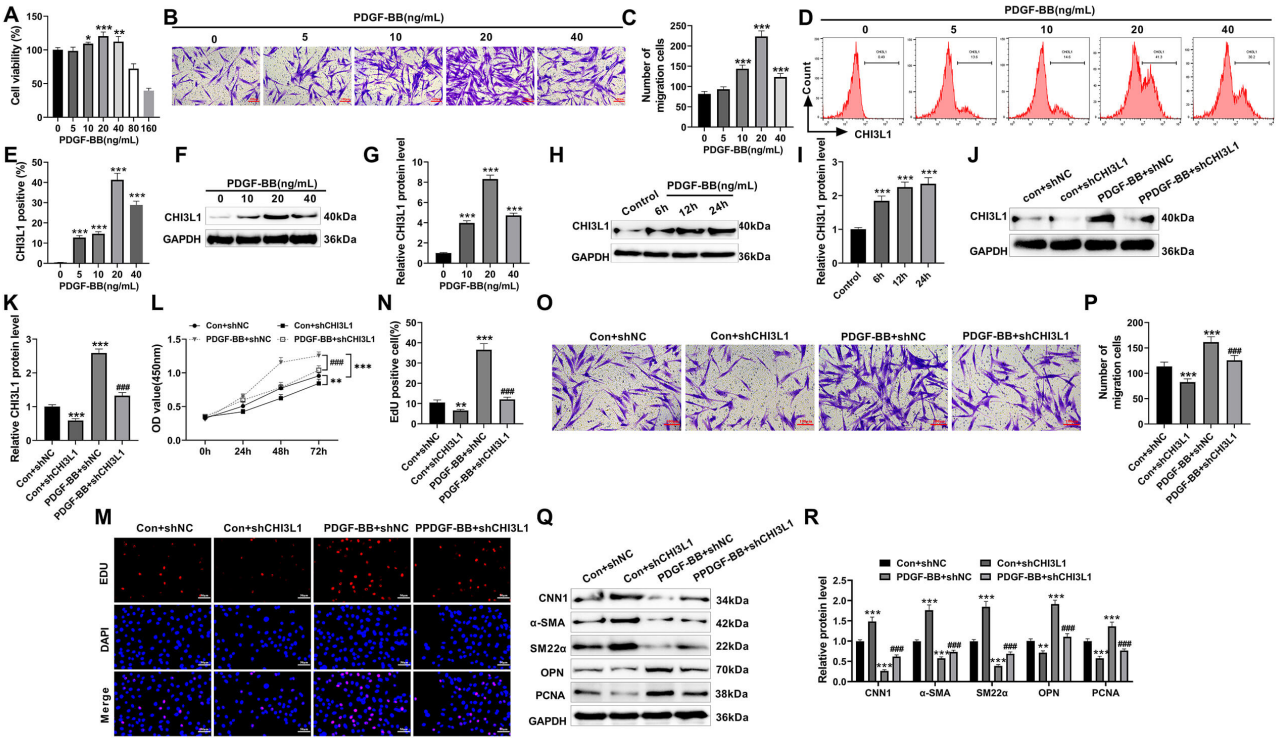

Fig. 2. Knockdown of CHI3L1 inhibits PDGF-BB–induced VSMC proliferation, migration, and dedifferentiation. (A) Assessment of PDGF-BB dose-dependent proliferation (CCK-8). (B,C) Evaluation of PDGF-BB-stimulated migration (Transwell; 20×, 100 μm). (D,E) Measurement of CHI3L1-positive cell proportion (Flow cytometry). (F–I) Examination of PDGF-BB-induced CHI3L1 expression (Western blot). * $p < 0.05$, ** $p < 0.01$, *** $p < 0.001$ vs Control. (J,K) Validation of CHI3L1 knockdown efficiency (Western blot) across four experimental groups. (L–N) Assessment of proliferative capacity (CCK-8 and EdU; 40×, 50 μm). (O,P) Evaluation of migratory capacity (Transwell; 20×, 100 μm). (Q,R) Detection of phenotypic markers (Western blot). n = 6. ** $p < 0.01$, *** $p < 0.001$ vs Con+shNC; ### $p < 0.001$ vs PDGF-BB+ shNC. PDGF-BB, Platelet-derived growth factor-BB; VSMC, vascular smooth muscle cell; CCK-8, Cell Counting Kit-8; EdU, 5-ethynyl-2′-deoxyuridine.

Knockdown of CHI3L1 Attenuates PDGF-BB–Induced Inflammatory Responses in VSMCs

Inflammatory responses also influence the pathological activation of VSMCs [33]. ICAM-1 and MCP-1 are key inflammatory molecules involved in diseases such as AS and vascular inflammation [34], which promote inflammatory cell infiltration, and their expression is regulated by inflammatory stimuli [35]. To elucidate CHI3L1's function in VSMC inflammation, inflammatory mediators were quantified. PDGF-BB treatment robustly enhanced the production and secretion of multiple inflammatory factors (TNF-α, IL-6, and IL-1β), and increased the protein levels of ICAM-1 and MCP-1 (Fig. 4A–H; $p < 0.001$). These pro-inflammatory effects were significantly attenuated by CHI3L1 knockdown, as evidenced by reduced levels of secreted cytokines and diminished expression of ICAM-1 and MCP-1 compared to the PDGF-BB+shNC group. Under basal conditions, CHI3L1 silencing alone did not alter these inflammatory markers ($p > 0.05$).

CHI3L1 Knockdown Attenuates PDGF-BB-Induced VSMC Proliferation, Migration, and Dedifferentiation via the JNK/ERK Pathway

To further elucidate the role of the JNK/ERK pathway in CHI3L1-mediated regulation of VSMC function, Western blot analysis showed that CHI3L1 knockdown markedly reduced the phosphorylation levels of JNK and ERK induced by PDGF-BB (Fig. 5A,B; $p < 0.001$). CCK-8 assays demonstrated that Anisomycin had no obvious cytotoxicity on VSMCs at relatively low concentrations (≤20 ng/mL, $p > 0.05$) (Fig. 5C). We then screened for the optimal concentration of Anisomycin that maximally activated JNK phosphorylation, when used alone (Fig. 5D,E; $p < 0.001$) or in combination with PDGF-BB (Fig. 5F,G; $p < 0.001$), and ultimately selected 20 ng/mL for subsequent experiments.

Cell viability assays revealed that CHI3L1 knockdown suppressed PDGF-BB-induced proliferation, and this inhibitory effect was partially reversed by Anisomycin (Fig. 5H; $p < 0.001$). Western blot analysis confirmed that Anisomycin restored the phosphorylation levels of JNK and

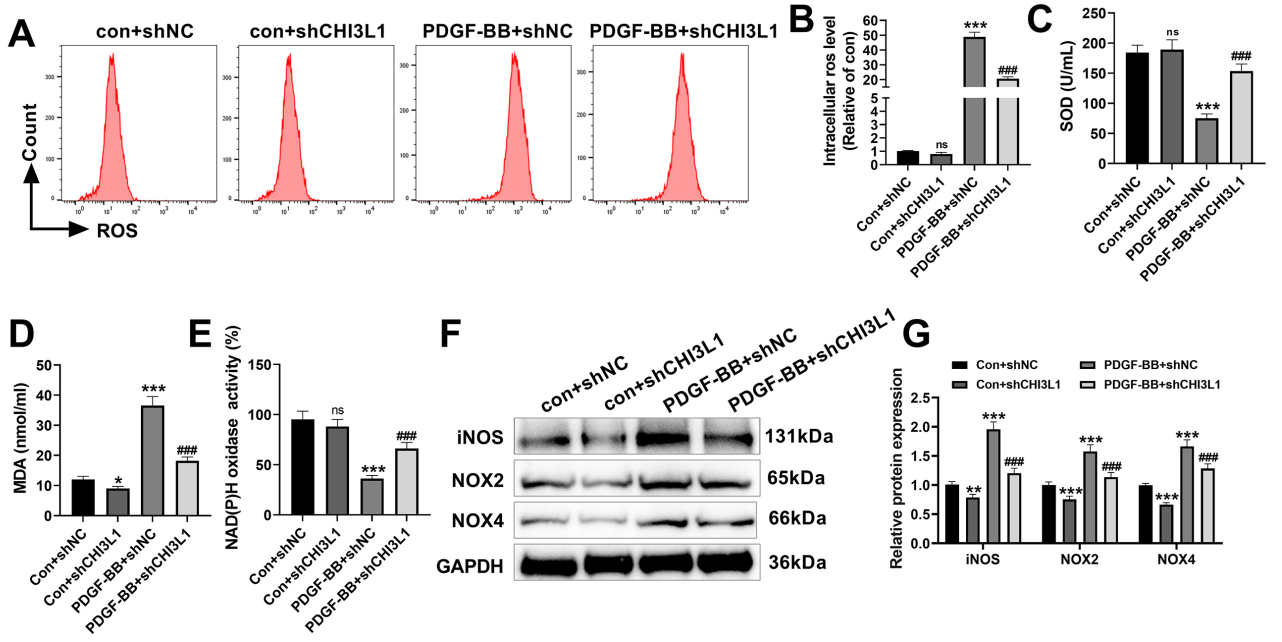

Fig. 3. Knockdown of CHI3L1 reduces PDGF-BB–induced oxidative stress in VSMCs. (A,B) Intracellular ROS in VSMCs. (C–E) Oxidative stress markers in VSMCs. (F,G) Expression of iNOS, NOX2, NOX4 in VSMCs. n = 6. ns $p > 0.05$, * $p < 0.05$, ** $p < 0.01$, *** $p < 0.001$ vs Con+shNC; ### $p < 0.001$ vs PDGF-BB+shNC. ROS, reactive oxygen species; NOX2, NADPH oxidase 2.

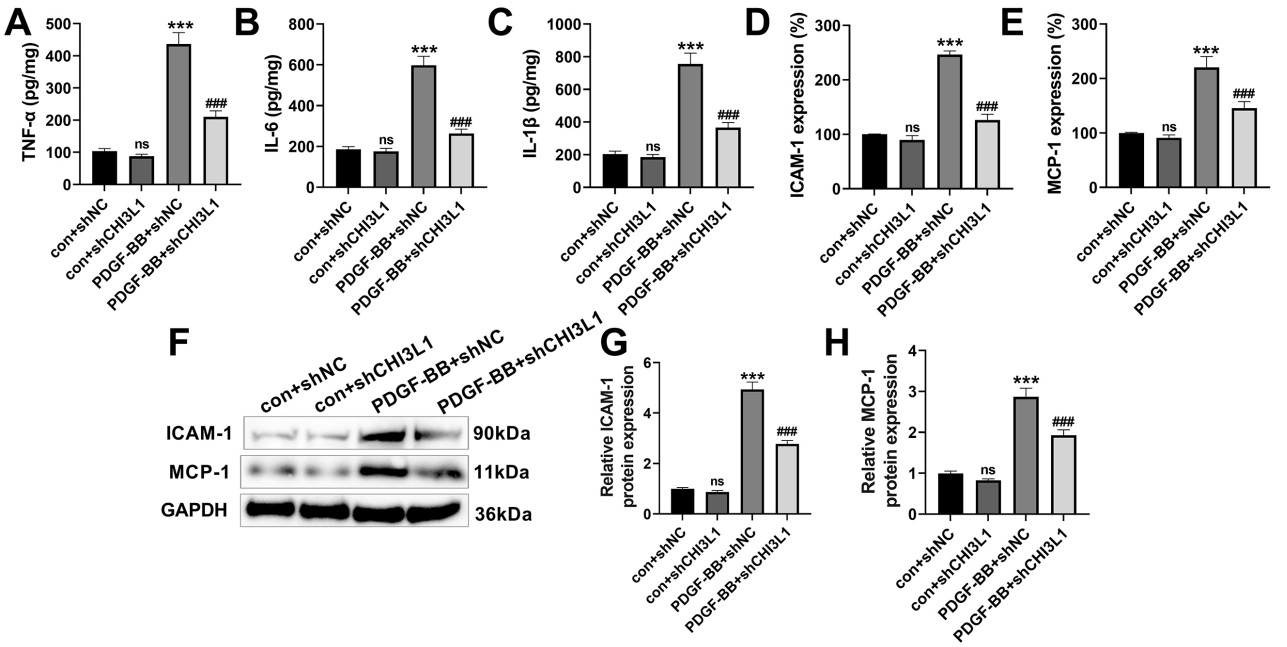

Fig. 4. Knockdown of CHI3L1 attenuates PDGF-BB–induced inflammatory responses in VSMCs. (A–C) ELISA of inflammatory cytokines (TNF-α, IL-6, IL-1β) in VSMC supernatants. (D–H) ELISA and Western blot analysis of ICAM-1 and MCP-1 in VSMCs. n = 6. ns $p > 0.05$, *** $p < 0.001$ vs con+shNC; ### $p < 0.001$ vs PDGF-BB+shNC. ELISA, Enzyme-Linked Immunosorbent Assay; TNF-α, Tumor Necrosis Factor-α; IL-6, Interleukin-6; ICAM-1, Intercellular Adhesion Molecule 1; MCP-1, Monocyte Chemoattractant Protein 1.

ERK that had been reduced by CHI3L1 knockdown (Fig. 5I,J). EdU staining (Fig. 5K,L) and Transwell migration assays (Fig. 5M,N) showed that the suppressive effects of CHI3L1 knockdown on PDGF-BB-induced VSMC proliferation and migration were significantly weakened after co-treatment with Anisomycin ($p < 0.001$). IF stain-

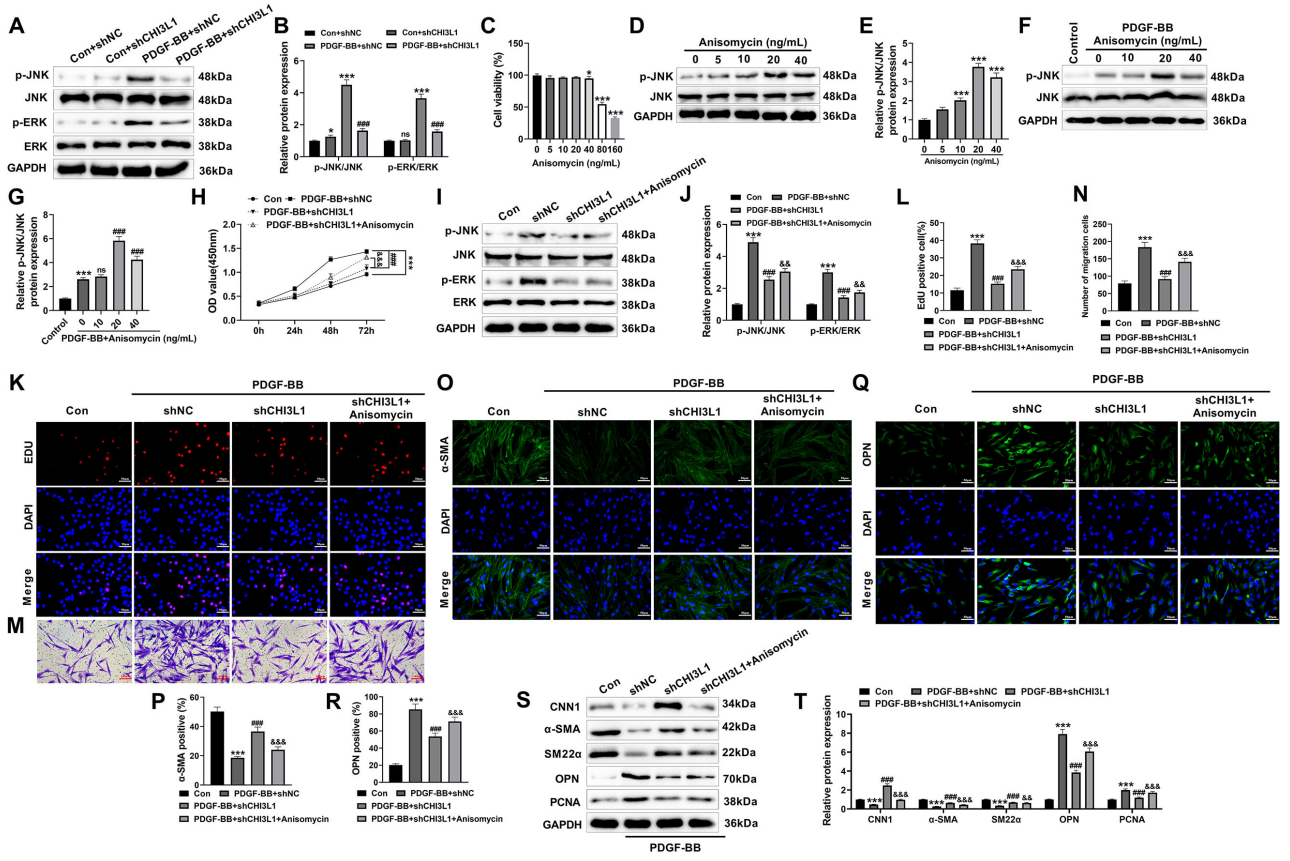

Fig. 5. CHI3L1 knockdown attenuates PDGF-BB-induced VSMC proliferation, migration, and dedifferentiation via the JNK/ERK pathway. (A,B) Western blot was used to analyze the phosphorylation levels of JNK (p-JNK/JNK) and ERK (p-ERK/ERK) in vascular smooth muscle cells of each group. ns $p > 0.05$, * $p < 0.05$, *** $p < 0.001$ vs Con+shNC; ### $p < 0.001$ vs PDGF-BB+shNC. (C) CCK-8 assay assessing the effects of different concentrations of Anisomycin (0, 5, 10, 20, 40, 80, 160 ng/mL) on VSMC viability. (D–G) Western blot screening for the optimal effective concentration of Anisomycin and assessing its impact on JNK signaling in PDGF-BB-stimulated VSMCs. ns $p > 0.05$, *** $p < 0.001$ vs Control; ### $p < 0.001$ vs PDGF-BB. (H) CCK-8 assay assessing proliferative activity of VSMCs in the following groups: control, PDGF-BB+shNC, PDGF-BB+shCHI3L1, PDGF-BB+shCHI3L1+20 ng/mL Anisomycin. (I,J) Western blot analysis of p-JNK, JNK, p-ERK, and ERK protein levels in the above groups. (K,L) EdU staining for VSMC proliferation in each group (40×, 50 μm). (M,N) Transwell assays for VSMC migration in each group (20×, 100 μm). (O–R) IF staining of α-SMA and OPN expression (40×, 50 μm). (S,T) Western blot analysis of differentiation markers (CNN1, α-SMA, SM22α), dedifferentiation marker (OPN), and proliferation marker (PCNA) in VSMCs from each group. n = 6. *** $p < 0.001$ vs Control; ### $p < 0.001$ vs PDGF-BB+shNC; && $p < 0.01$, &&& $p < 0.001$ vs PDGF-BB+ shCHI3L1. JNK, c-Jun N-terminal kinase; ERK, extracellular signal-regulated kinase; CNN1, calponin 1.

ing indicated that CHI3L1 knockdown partially restored the PDGF-BB-induced decrease in the expression of the contractile protein α-SMA and reduced the expression of the synthetic protein OPN, while the addition of Anisomycin reversed these effects of CHI3L1 knockdown (Fig. 5O–R; $p < 0.001$). Western blot analysis revealed that knockdown of CHI3L1 upregulated the expression of contractile phenotype markers (CNN1, α-SMA, and SM22α), while downregulating the expression of the dedifferentiation marker OPN and the proliferation marker PCNA ($p < 0.001$). Notably, activation of the JNK pathway by anisomycin partially reversed the aforementioned alterations in marker expression induced by CHI3L1 knockdown (Fig. 5S,T). These findings indicate that CHI3L1 knockdown suppresses PDGF-BB-induced activation of the JNK and ERK signaling pathways. Pharmacological re-activation of the JNK pathway partially abrogates the inhibitory effects of CHI3L1 knockdown on VSMC proliferation, migration, and transition to a synthetic phenotype.

CHI3L1 Knockdown Attenuates PDGF-BB-Induced VSMC Inflammation and Oxidative Stress via the JNK/ERK Pathway

To determine whether the JNK/ERK pathway mediates the inhibitory effects of CHI3L1 knockdown on PDGF-BB-induced oxidative stress and inflammatory responses,

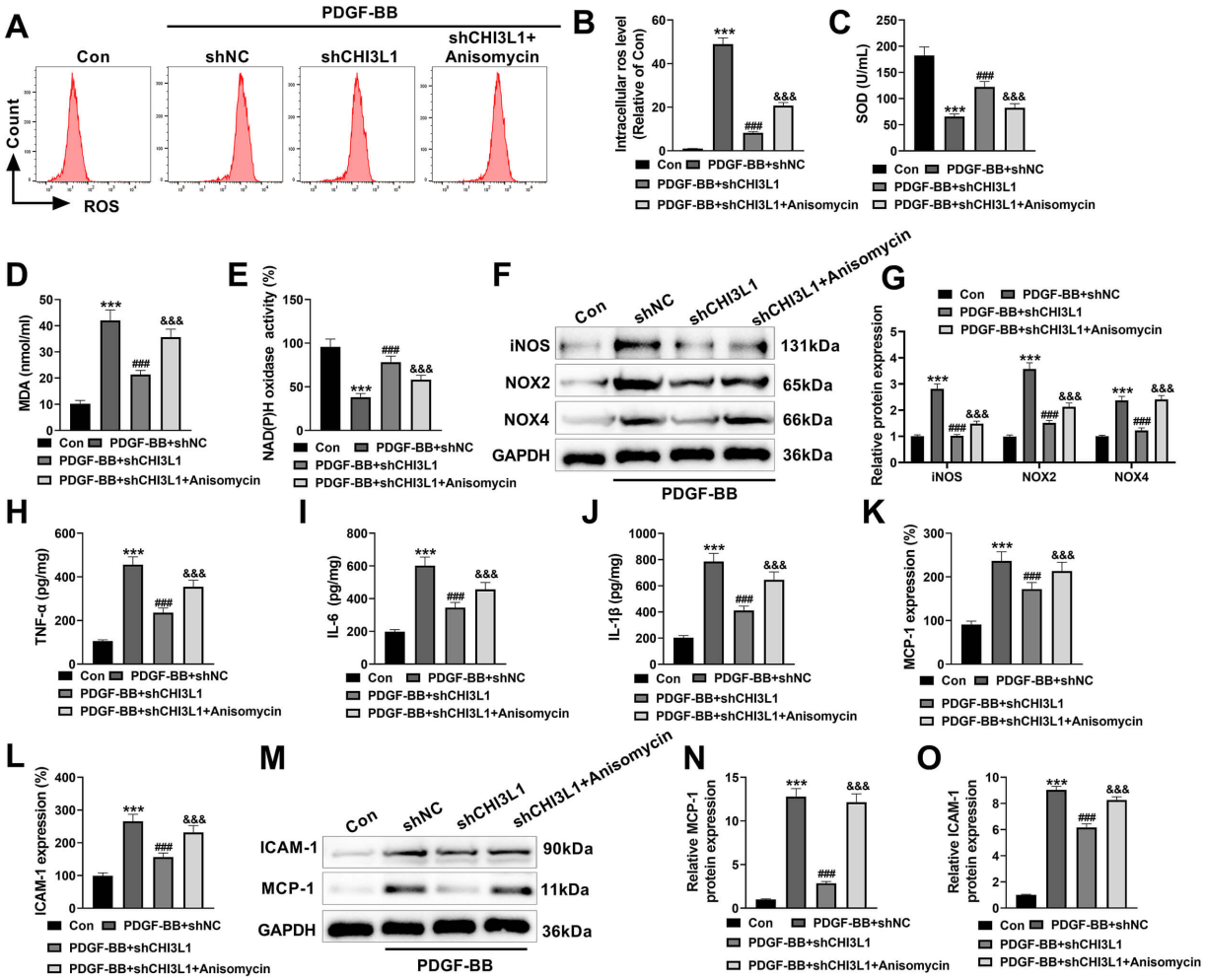

Fig. 6. CHI3L1 knockdown attenuates PDGF-BB-induced VSMC inflammation and oxidative stress via the JNK/ERK pathway. (A,B) Detection of ROS levels in VSMCs by flow cytometry. (C–E) Assessment of oxidative stress indices in VSMCs. (F,G) Evaluation of iNOS, NOX2, and NOX4 expression in VSMCs via Western blot. (H–J) Quantification of TNF-α, IL-6, and IL-1β in VSMC supernatants using ELISA. (K–O) Analysis of ICAM-1 and MCP-1 levels in VSMCs by combined ELISA and Western blot. n = 6. *** $p < 0.001$ vs Con; ### $p < 0.001$ vs PDGF-BB+shNC; &&& $p < 0.001$ vs PDGF-BB+ shCHI3L1.

we performed rescue experiments using the JNK agonist Anisomycin. With respect to oxidative stress, compared with the PDGF-BB+NC group, CHI3L1 knockdown reduced intracellular ROS and MDA levels and increased SOD activity and NAD(P)H levels (Fig. 6A–E; $p < 0.001$). These beneficial effects were attenuated by Anisomycin treatment. CHI3L1 knockdown inhibited PDGF-BB-induced upregulation of iNOS, NOX2, and NOX4 expression (Fig. 6F,G; $p < 0.001$), and this suppression was likewise partially reversed by Anisomycin.

Regarding inflammation, CHI3L1 knockdown decreased the levels of TNF-α, IL-6, and IL-1β secreted by VSMCs in response to PDGF-BB stimulation (Fig. 6H–J; $p < 0.001$), whereas Anisomycin treatment increased the secretion of these pro-inflammatory cytokines. Moreover, CHI3L1 knockdown downregulated PDGF-BB-induced ICAM-1 and MCP-1 expression (Fig. 6K–O; $p < 0.001$), and co-treatment with Anisomycin weakened this downregulation. These data indicate that the ameliorative effects of CHI3L1 knockdown on PDGF-BB-induced oxidative stress and inflammatory responses can be reversed by re-activation of the JNK pathway. This further supports that CHI3L1 influences redox homeostasis and inflammatory responses in VSMCs by modulating the downstream JNK/ERK pathway.

CHI3L1 Knockdown Alleviates VIH in Rats by Inhibiting Vascular Inflammation and Oxidative Stress via the JNK/ERK Pathway

To validate *in vivo* the role of CHI3L1 in regulating vascular inflammation, oxidative stress, and IH via the JNK/ERK pathway, we performed adenovirus-mediated

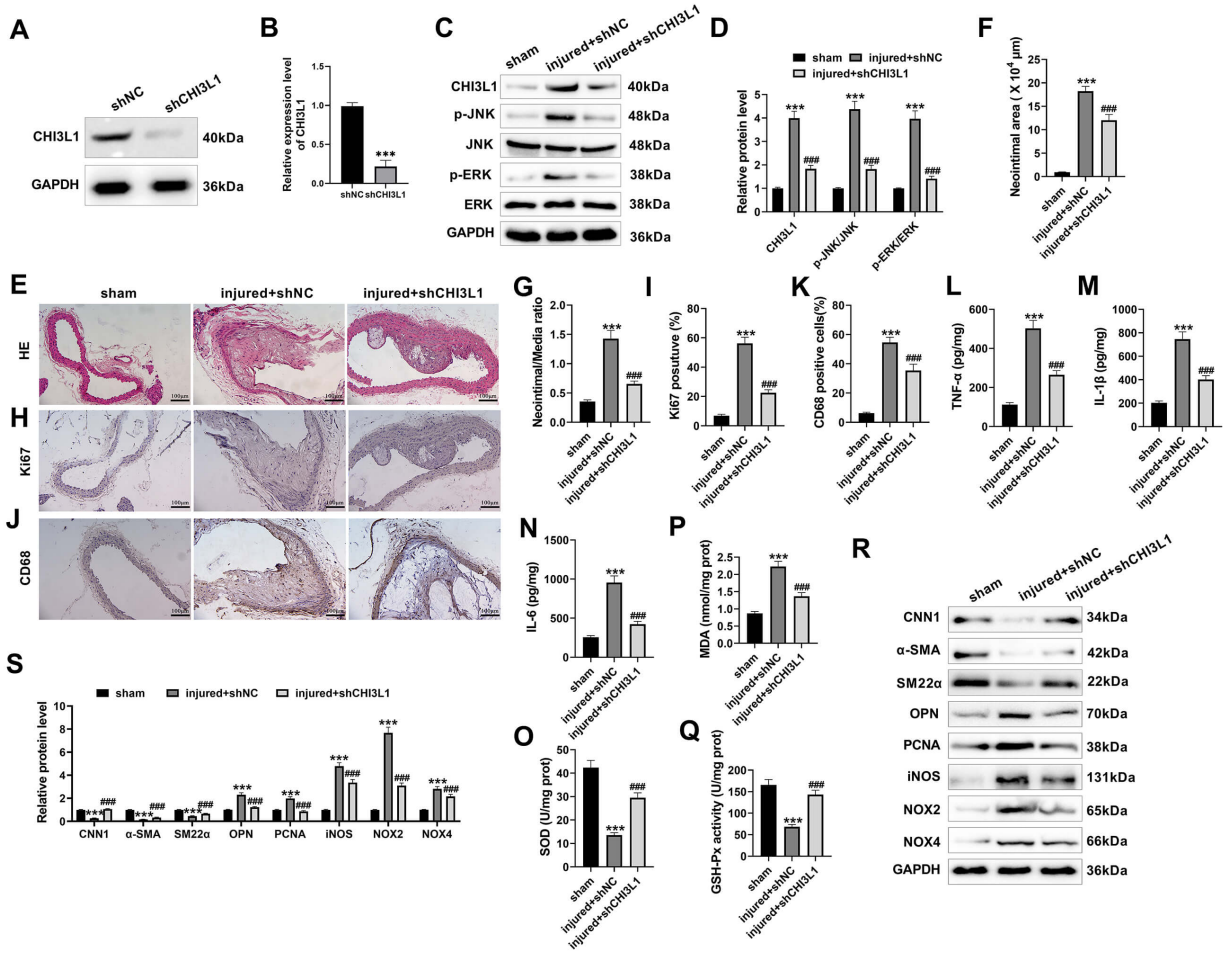

Fig. 7. Knockdown of CHI3L1 attenuates rat VIH by inhibiting vascular inflammation and oxidative stress via the JNK/ERK pathway. (A,B) Western blot detection of venous CHI3L1 knockdown efficiency. (C,D) Western blot analysis of CHI3L1, p-JNK/JNK, and p-ERK/ERK protein expression in venous tissues. (E–G) HE staining of venous tissues and quantitative analysis of neointimal area and intima-to-media ratio in each group (20×, 100 μm). (H–K) Immunohistochemical staining of Ki67 and CD68 in venous tissues to assess cell proliferation and macrophage infiltration (20×, 100 μm). (L–N) Measurement of serum levels of the inflammatory cytokines TNF-α, IL-6, and IL-1β. (O–Q) Detection of oxidative stress indices in venous tissues: SOD activity and MDA and GSH-Px contents. (R,S) Western blot detection of CNN1, α-SMA, SM22α, OPN, PCNA, iNOS, NOX2, and NOX4 protein expression levels in venous tissues. n = 9 biological replicates *in vivo* per group. *** $p < 0.001$ vs Sham; ### $p < 0.001$ vs injured+shNC.

CHI3L1 knockdown in AVF model rats (Fig. 7A,B; $p < 0.001$). Western blot analysis at 21 days post-operation showed that CHI3L1 protein expression was markedly up-regulated in venous tissues of the injured+shNC group, accompanied by a pronounced increase in JNK and ERK phosphorylation (Fig. 7C,D; $p < 0.001$). In contrast, these changes were effectively reversed in the injured+shCHI3L1 group, as evidenced by decreased CHI3L1 expression and concomitant reductions in p-JNK and p-ERK levels ($p < 0.001$). This indicates that *in vivo* CHI3L1 knockdown also inhibits AVF-induced activation of the JNK/ERK signaling pathway.

HE staining revealed prominent neointimal IH at the venous anastomosis in the injured+shNC group compared with the sham group, whereas the injured+shCHI3L1 group exhibited significantly reduced neointimal thickness, intima-to-media area ratio, and total neointimal area (Fig. 7E–G; $p < 0.001$), suggesting that CHI3L1 knockdown effectively suppresses NIH progression in rats. Meanwhile, IHC staining showed that the Ki67-positive cell rate was markedly higher in the injured+shNC group than in the sham group, while CHI3L1 knockdown significantly reduced cell proliferation (Fig. 7H,I; $p < 0.001$). CD68-positive macrophage infiltration in the venous wall was markedly increased in the injured+shNC group and was reduced by CHI3L1 knockdown (Fig. 7J,K; $p < 0.001$). ELISA assays further showed elevated serum levels of pro-inflammatory cytokines in the injured+shNC rats, which were reduced by CHI3L1 knockdown (Fig. 7L–N; $p < 0.001$). Regarding oxidative stress, compared with the in-

jured+shNC group, CHI3L1 knockdown partially restored SOD activity and GSH-Px content in venous tissue, while reducing MDA levels (Fig. 7O–Q; $p < 0.001$). CHI3L1 knockdown upregulated the expression of contractile markers (CNN1, α-SMA, SM22α) and downregulated the expression of the synthetic marker OPN, the proliferation marker PCNA, and pro-oxidant proteins (iNOS, NOX2, NOX4) (Fig. 7R,S; $p < 0.001$). Collectively, these results demonstrate that CHI3L1 knockdown effectively inhibits activation of the JNK/ERK signaling pathway at the venous anastomosis in AVF model rats, reduces local inflammatory cell infiltration and inflammatory mediator levels, improves redox imbalance, and ultimately alleviates VIH.

Discussion

VIH is a key pathological process leading to early failure of AVF and stenosis of hemodialysis access [36]. Driven by hemodynamic alterations and surgical injury following AVF creation, the vessel wall undergoes intense pathological remodeling, in which phenotypic switching, excessive proliferation, and migration of VSMCs play pivotal roles [37]. In this study, using a rat AVF model, we found that CHI3L1 expression was markedly upregulated in venous fistula tissues and positively correlated with neointimal area and the extent of macrophage infiltration. This finding is highly consistent with recent studies on the role of CHI3L1 in cardiovascular remodeling [38]. As a pro-inflammatory cytokine, CHI3L1 plays an important role in tissue injury repair and chronic inflammation [39]. Previous studies have demonstrated that serum CHI3L1 levels are an independent risk factor for early AVF failure in uremic patients [40] and is highly expressed in vulnerable atherosclerotic plaques [41]. Our experimental results further confirm the critical role of CHI3L1 in VIH, suggesting that it is not only a biomarker of vascular injury, but also an important regulator of venous pathological remodeling.

In this study, we further explored the molecular mechanisms by which CHI3L1 regulates VSMC function using an *in vitro* PDGF-BB–induced VSMC activation model. We found that CHI3L1 knockdown significantly inhibited VSMC proliferation, migration, and phenotypic switch from a contractile to a synthetic state. Phenotypic transition of VSMCs is the initiating event of vascular remodeling. Synthetic VSMCs exhibit stronger proliferative and secretory capacities and can produce large amounts of ECM, ultimately leading to luminal narrowing [42,43]. Evidence indicates that CHI3L1 exerts its effects via the MAPK pathway in various inflammatory diseases [44]. Our study further demonstrated that CHI3L1 knockdown markedly reduced PDGF-BB–induced phosphorylation of JNK and ERK, whereas application of the JNK agonist Anisomycin partially reversed the inhibitory effects of CHI3L1 knockdown on VSMC proliferation and phenotypic switching. Although anisomycin is commonly used as a JNK pathway activator, it may also influence other stress-related signaling cascades; therefore, our data support the involvement of the JNK/ERK axis rather than proving absolute pathway specificity. These findings nevertheless suggest that activation of the JNK/ERK signaling pathway is an important link in the pro-proliferative effect of CHI3L1. The ERK pathway mainly regulates cell cycle progression and protein synthesis [45], while the JNK pathway is closely associated with oxidative stress responses and cell migration [46]. The two pathways act synergistically to drive the pathological activation of VSMCs.

CHI3L1 in vascular pathology is context-dependent. Although this study clarified its pro-inflammatory and pro-proliferative effects in the AVF model, there are also reports that CHI3L1 may exhibit anti-inflammatory potential under certain immune conditions. For example, in sepsis, CHI3L1 can limit tissue damage and promote repair by driving macrophage polarization toward the M2 phenotype [47]. However, in the pathological process of AVF, the pro-inflammatory effects of CHI3L1 clearly predominate. This “double-edged sword” phenomenon suggests that the function of CHI3L1 may depend on the repertoire of receptors it engages and the local microenvironment. In addition, the interaction between vascular endothelial cells and VSMCs is likewise non-negligible in the progression of IH. CHI3L1 not only acts directly on VSMCs, but may also exacerbate vascular remodeling by inducing endothelial-to-mesenchymal transition in endothelial cells. According to recent research, CHI3L1 engages the CD44 receptor to trigger mTORC1 pathway activation [48]. This, in turn, drives endothelial cells to undergo endothelial-to-mesenchymal transition (EndMT), a key event in the development of neointima. In the AVF model, injured endothelial cells release CHI3L1, which not only induces VSMC phenotypic switching through paracrine signaling, but may also undergo EndMT themselves to transform into fibroblast-like cells; this dual mechanism jointly accelerates luminal occlusion.

Inflammatory responses and oxidative stress are the two major driving forces behind VSMC phenotypic switching and IH progression. We found that CHI3L1 knockdown markedly reduced TNF-α, IL-6, IL-1β, MCP-1, ICAM-1 expression in VSMCs. CHI3L1 *per se* has chemotactic effects on macrophages and promotes inflammatory infiltration; its high expression in the vascular wall can shape a pro-inflammatory microenvironment that further drives the transition of VSMCs toward the synthetic phenotype. At the same time, oxidative stress is likewise a critical component of CHI3L1-mediated vascular injury. Our data showed that CHI3L1 knockdown effectively suppressed ROS generation, reduced MDA levels, and increased SOD activity. Mechanistically, CHI3L1 maintains intracellular redox homeostasis by regulating the expression of iNOS and NADPH oxidase isoforms NOX2 and NOX4. The NOX family proteins are the main source of ROS in the vascu-

lar wall, and their activation is tightly controlled by the MAPK pathway [49]. When CHI3L1 is silenced, the inhibition of the JNK/ERK pathway leads to downregulation of NOX2/4 expression, thereby attenuating oxidative stress–induced cellular injury. Under the control of CHI3L1, the interplay between inflammation and oxidative stress forms a vicious cycle: inflammatory mediators induce ROS production, whereas ROS, in turn, amplify the inflammatory response by activating redox-sensitive transcription factors, ultimately synergistically driving excessive VIH.

In the *in vivo* experiments, adenovirus-mediated CHI3L1 knockdown significantly attenuated intimal thickening in the rat AVF model and ameliorated inflammatory infiltration and oxidative damage in the vascular wall. The identification of CHI3L1's critical role in IH pathogenesis represents a significant finding, underscoring its potential as a novel therapeutic target. To further validate the generalizability of CHI3L1's effects, future studies could perform multi-model verification using, for example, AS models or carotid artery ligation models. Human studies have already shown that serum CHI3L1 levels correlate closely with the severity of coronary artery disease [50], implying considerable potential for translation from animal models to clinical practice. Interventions targeting CHI3L1 should carefully consider both timing and delivery strategy. Our data suggest that early intervention after AVF creation (e.g., within 7 days postoperatively) may yield optimal preventive effects by suppressing the early inflammatory cascade. Compared with systemic administration, local drug delivery (such as drug-coated balloons or perivascular slow-release gels) can achieve higher local concentrations with fewer systemic side effects and thus represents a key direction for future clinical translation [51]. Combining CHI3L1-targeted therapy with existing antiplatelet agents or statins may produce synergistic effects and further improve long-term patency of dialysis access.

Conclusion

In summary, knockdown of CHI3L1 can significantly inhibit activation of the JNK/ERK signaling pathway, attenuate vascular wall inflammatory responses and oxidative stress, thereby blocking the pathological phenotypic switching, excessive proliferation, and migration of VSMCs, and ultimately alleviating AVF-related VIH. Although CHI3L1 may exert complex biological functions under different contexts, its role as a pro-inflammatory and pro-proliferative factor in pathological vascular remodeling is well established. Future studies should further elucidate the intricate crosstalk between CHI3L1 and the immune system, particularly its precise role in immune cell recruitment, and develop more comprehensive, multi-targeted intervention strategies, with the aim of providing new approaches for long-term maintenance of vascular access in hemodialysis patients.

Abbreviations

MDA, Malondialdehyde; ROS, Reactive Oxygen Species; GSH-Px, Glutathione Peroxidase; VSMC, vascular smooth muscle cell; VIH, Venous Intimal Hyperplasia; AVF, Arteriovenous Fistula; IH, Intimal Hyperplasia; NIH, neointimal hyperplasia; ECM, Extracellular Matrix; CHI3L1, Chitinase-3-Like Protein 1; JNK, c-Jun N-terminal Kinase; ERK, Extracellular Signal-Regulated Kinase; MAPK, Mitogen-Activated Protein Kinase; PDGF-BB, Platelet-Derived Growth Factor-BB; CFA, common femoral artery; SEV, superficial epigastric vein; HE, Hematoxylin and Eosin; IHC, Immunohistochemistry; IF, Immunofluorescence; ELISA, Enzyme-Linked Immunosorbent Assay; SOD, Superoxide Dismutase; NAD(P)H, Reduced Nicotinamide Adenine Dinucleotide Phosphate; TNF-α, Tumor Necrosis Factor-α; IL-6, Interleukin-6; IL-1β, Interleukin -1β; ICAM-1, Intercellular Adhesion Molecule 1; MCP-1, Monocyte Chemoattractant Protein 1; α-SMA, α- Smooth Muscle Actin; OPN, Osteopontin; CNN1, Calponin 1; EndMT, endothelial-to-mesenchymal transition; SM22α, Smooth muscle protein 22α; PCNA, Proliferating Cell Nuclear Antigen; NOX4, NADPH Oxidase 4; NOX2, NADPH Oxidase 2.

Availability of Data and Materials

The datasets used or analyzed during the current study are available from the corresponding author upon reasonable request.

Author Contributions

XBC conceived and designed the study, conducted the experiments, analyzed the data, and drafted and critically revised the manuscript for important intellectual content. SSY contributed to data acquisition, analysis, and interpretation and provided substantial intellectual input during the drafting and revision of the manuscript. JX and FLY participated in the conception and design of the study and contributed substantially to data interpretation and manuscript preparation and revision. All authors gave final approval of the version to be published. All authors have participated sufficiently in the work to take public responsibility for appropriate portions of the content and agreed to be accountable for all aspects of the work in ensuring that questions related to its accuracy or integrity.

Ethics Approval and Consent to Participate

All animal experiments were approved by the Zhejiang Free Trade Zone Ruisai Biopharmaceutical Technology Limited Company Experimental Animal Welfare and Ethics Committee Ethics Committee (Approval Number: 2024073179). All procedures complied with the ARRIVE Guidelines 2.0.

Acknowledgment

Not applicable.

Funding

This research was supported by the Zhejiang Medical and Health Science and Technology Project (NO. 2022KY1364) and Zhoushan Medical and Health Science and Technology Project (NO. 2022YA08).

Conflict of Interest

The authors declare no conflict of interest.

References

[1] Vazquez-Padron RI, Duque JC, Tabbara M, Salman LH, Martinez L. Intimal Hyperplasia and Arteriovenous Fistula Failure: Looking Beyond Size Differences. Kidney360. 2021; 2: 1360–1372. https://doi.org/10.34067/KID.0002022021

[2] Sahasrabudhe P, Bindu A. Nuances of Arteriovenous Fistula Creation for Vascular Access in Hemodialysis. Indian Journal of Plastic Surgery : Official Publication of the Association of Plastic Surgeons of India. 2021; 54: 257–263. https://doi.org/10.1055/s-0041-1734576

[3] Kaller R, Russu E, Arbănași EM, Mureșan AV, Jakab M, Ciucanu CC, et al. Intimal CD31-Positive Relative Surfaces Are Associated with Systemic Inflammatory Markers and Maturation of Arteriovenous Fistula in Dialysis Patients. Journal of Clinical Medicine. 2023; 12: 4419. https://doi.org/10.3390/jcm12134419

[4] Barcena AJR, Perez JVD, Liu O, Mu A, Heralde FM, 3rd, Huang SY, et al. Localized Perivascular Therapeutic Approaches to Inhibit Venous Neointimal Hyperplasia in Arteriovenous Fistula Access for Hemodialysis Use. Biomolecules. 2022; 12: 1367. https://doi.org/10.3390/biom12101367

[5] Ji Z, Li J, Wang J. Jujuboside B Inhibits Neointimal Hyperplasia and Prevents Vascular Smooth Muscle Cell Dedifferentiation, Proliferation, and Migration *via* Activation of AMPK/PPAR-γ Signaling. Frontiers in Pharmacology. 2021; 12: 672150. https://doi.org/10.3389/fphar.2021.672150

[6] Totoń-Żurańska J, Mikolajczyk TP, Saju B, Guzik TJ. Vascular remodelling in cardiovascular diseases: hypertension, oxidation, and inflammation. Clinical Science (London, England : 1979). 2024; 138: 817–850. https://doi.org/10.1042/CS20220797

[7] Xu X, Xie L, Chai L, Wang X, Dong J, Wang J, et al. Ketogenic diet inhibits neointimal hyperplasia by suppressing oxidative stress and inflammation. Clinical and Experimental Hypertension (New York, N.Y. : 1993). 2023; 45: 2229538. https://doi.org/10.1080/10641963.2023.2229538

[8] Dong Z-F, Long Y, Sun W-J, Wang Y, Huang Y-H, Wang G-X, et al. Role of smooth muscle progenitor cells in vascular mechanical injury and repair. Medicine in Novel Technology and Devices. 2022; 16: 100178.

[9] Akhigbe R, Ajayi A. The impact of reactive oxygen species in the development of cardiometabolic disorders: a review. Lipids in Health and Disease. 2021; 20: 23. https://doi.org/10.1186/s12944-021-01435-7

[10] Hu K, Guo Y, Li Y, Lu C, Cai C, Zhou S, et al. Oxidative stress: An essential factor in the process of arteriovenous fistula failure. Frontiers in Cardiovascular Medicine. 2022; 9: 984472. https://doi.org/10.3389/fcvm.2022.984472

[11] Zhao H, Huang M, Jiang L. Potential Roles and Future Perspectives of Chitinase 3-like 1 in Macrophage Polarization and the Development of Diseases. International Journal of Molecular Sciences. 2023; 24: 16149. https://doi.org/10.3390/ijms242216149

[12] Mizoguchi E, Wang S. Future Perspectives and Conclusions from Animal Models of CHI3L1-Related Inflammation-Associated Cancer. Cells. 2025; 14: 982. https://doi.org/10.3390/cells14130982

[13] Sun X, Nakajima E, Norbrun C, Sorkhdini P, Yang AX, Yang D, et al. Chitinase 3 like 1 contributes to the development of pulmonary vascular remodeling in pulmonary hypertension. JCI Insight. 2022; 7: e159578. https://doi.org/10.1172/jci.insight.159578

[14] Zhu Y, Chen JC, Zhang JL, Wang FF, Liu RP. A new mechanism of arterial calcification in diabetes: interaction between H3K18 lactylation and CHI3L1. Clinical Science (London, England : 1979). 2025; 139: 115–130. https://doi.org/10.1042/CS20243122

[15] Tsantilas P, Lao S, Wu Z, Eberhard A, Winski G, Vaerst M, et al. Chitinase 3 like 1 is a regulator of smooth muscle cell physiology and atherosclerotic lesion stability. Cardiovascular Research. 2021; 117: 2767–2780. https://doi.org/10.1093/cvr/cvab014

[16] Chang MC, Chen CT, Chiang PF, Chiang YC. The Role of Chitinase-3-like Protein-1 (YKL40) in the Therapy of Cancer and Other Chronic-Inflammation-Related Diseases. Pharmaceuticals (Basel, Switzerland). 2024; 17: 307. https://doi.org/10.3390/ph17030307

[17] Zhang L, Wang Z, Li S, Liu X, Xu C, Li L. The Potential Roles of CHI3L1 in Failed Autologous Arteriovenous Fistula in End-Stage Renal Disease. The Tohoku Journal of Experimental Medicine. 2023; 259: 253–261. https://doi.org/10.1620/tjem.2022.J120

[18] Wen X, Jiao L, Tan H. MAPK/ERK Pathway as a Central Regulator in Vertebrate Organ Regeneration. International Journal of Molecular Sciences. 2022; 23: 1464. https://doi.org/10.3390/ijms23031464

[19] Zhang J, Xu J, Burong H. Mitochondria and Tumorigenesis. Journal of Cancer Biomoleculars and Therapeutics. 2025; 2: 37–53. https://doi.org/10.62382/jcbt.v2i3.69

[20] Jia K, Shi P, Zhang L, Yan X, Xu J, Liao K. Trans-cinnamic acid alleviates high-fat diet-induced renal injury via JNK/ERK/P38 MAPK pathway. The Journal of Nutritional Biochemistry. 2025; 135: 109769. https://doi.org/10.1016/j.jnutbio.2024.109769

[21] Choi T, Lee JW, Kim SK, Yoo KH. Diabetes Mellitus Promotes Smooth Muscle Cell Proliferation in Mouse Ureteral Tissue through the P-ERK/P-JNK/VEGF/PKC Signaling Pathway. Medicina (Kaunas, Lithuania). 2021; 57: 560. https://doi.org/10.3390/medicina57060560

[22] Chen XY, Yang LP, Zheng YL, Li YX, Zhong DL, Jin RJ, et al. Electroacupuncture Attenuated Phenotype Transformation of Vascular Smooth Muscle Cells via PI3K/Akt and MAPK Signaling Pathways in Spontaneous Hypertensive Rats. Chinese Journal of Integrative Medicine. 2022; 28: 357–365. https://doi.org/10.1007/s11655-021-2883-y

[23] Hsuan CF, Kuo YT, Chang TH, Chen YL, Houng HY, Chang N, et al. *Abelmoschus manihot* Flower Extract Retards Platelet-Derived Growth Factor-BB-Stimulated Proliferation and Migration in Vascular Smooth Muscle Cells by Inhibiting the MAPK/NF-κB Pathway and Matrix Metalloproteinase Expressions. Journal of Medicinal Food. 2025; 28: 921–933. https://doi.org/10.1089/jmf.2024.k.0263

[24] Jin T, He P, Yang R, Geng R, Yang G, Xu Y. CHI3L1 promotes Staphylococcus aureus-induced osteomyelitis by activating p38/MAPK and Smad signaling pathways. Experimental Cell Research. 2021; 403: 112596. https://doi.org/10.1016/j.yexcr.2021.112596

[25] Somarathna M, Isayeva-Waldrop T, Al-Balas A, Guo L, Lee T. A Novel Model of Balloon Angioplasty Injury in Rat Arteriove-

nous Fistula. Journal of Vascular Research. 2020; 57: 223–235. https://doi.org/10.1159/000507080

[26] Zhang Y, Wu L, Liang L, Li K, Kong X, Wang H. Application of transthoracic echocardiography to assess the dynamic evolution of early cardiac damage induced by abdominal aorta-inferior vena cava fistula in female rats with chronic renal failure. PloS One. 2025; 20: e0324951. https://doi.org/10.1371/journal.pone.0324951

[27] Duan Y, Zhang Y, Qu C, Yu W, Tana, Shen C. CKLF1 aggravates neointimal hyperplasia by inhibiting apoptosis of vascular smooth muscle cells through PI3K/AKT/NF-κB signaling. Biomedicine & Pharmacotherapy = Biomedecine & Pharmacotherapie. 2019; 117: 108986. https://doi.org/10.1016/j.biopha.2019.108986

[28] Zhang T, Cao RJ, Niu JL, Chen ZH, Mu SQ, Cao T, et al. G6PD maintains the VSMC synthetic phenotype and accelerates vascular neointimal hyperplasia by inhibiting the VDAC1-Bax-mediated mitochondrial apoptosis pathway. Cellular & Molecular Biology Letters. 2024; 29: 47. https://doi.org/10.1186/s11658-024-00566-w

[29] Li H, Zhang H, Dai R, Zheng D, Zhao J, Jing H, et al. CD68 as a multi-omic prognostic biomarker in digestive system cancers: correlations with tumor-infiltrating immune cells and immune checkpoints. Frontiers in Immunology. 2025; 16: 1599677. https://doi.org/10.3389/fimmu.2025.1599677

[30] Zhang D, Cao Y, Liu D, Zhang J, Guo Y. The Etiology and Molecular Mechanism Underlying Smooth Muscle Phenotype Switching in Intimal Hyperplasia of Vein Graft and the Regulatory Role of microRNAs. Frontiers in Cardiovascular Medicine. 2022; 9: 935054. https://doi.org/10.3389/fcvm.2022.935054

[31] Delgadillo LF, Rashdan NA, Hamilton H, Pattillo JH, Yuan S, Eshaq RS, et al. Calcification in Vascular Smooth Muscle Cells Is Associated with Elevated GCLm and Impaired Contraction: Insights into Osteogenic Transdifferentiation and Therapeutic Approaches. Pathophysiology : the Official Journal of the International Society for Pathophysiology. 2025; 32: 66. https://doi.org/10.3390/pathophysiology32040066

[32] Xu S, Han X, Wang X, Yu Y, Qu C, Liu X, et al. The role of oxidative stress in aortic dissection: a potential therapeutic target. Frontiers in Cardiovascular Medicine. 2024; 11: 1410477. https://doi.org/10.3389/fcvm.2024.1410477

[33] Lopacinska N, Wesoly J, Bluyssen HAR. Interplay Between KLF4, STAT, IRF, and NF-κB in VSMC and Macrophage Plasticity During Vascular Inflammation and Atherosclerosis. International Journal of Molecular Sciences. 2025; 26: 10205. https://doi.org/10.3390/ijms262010205

[34] Zhao W, Wei H, Lu J, Sha W, Sun D, Pan T, et al. Tyrosol attenuates lipopolysaccharide-induced inflammation in HUVECs to promote vascular health against atherosclerosis challenge. Experimental and Therapeutic Medicine. 2023; 25: 240. https://doi.org/10.3892/etm.2023.11939

[35] Quarta S, Calabriso N, Carluccio MA, Lo Rizzo M, Wabitsch M, Verri T, et al. Anti-Inflammatory Role of Myo-Inositol in Obesity: Suppression of TNF-α-Induced Inflammation and Monocyte Adhesion in Hypertrophic Human Adipocytes. Food Science & Nutrition. 2025; 13: e70962. https://doi.org/10.1002/fsn3.70962

[36] Nguyen NT, Ingle KA, Waldrop TI, Lose BG, Collie PC, Gard WA, et al. Nitric Oxide-Releasing Nanomatrix Gel Inhibits Venous Intimal Hyperplasia and Improves Vascular Remodeling in Porcine Arteriovenous Fistula (AVF): FR-PO464. Journal of the American Society of Nephrology. 2023; 34: 530–531.

[37] Li Z, Zhao Y, Pan Z, Cai B, Zhang C, Jiao J. LncRNA-LncDACH1 mediated phenotypic switching of smooth muscle cells during neointimal hyperplasia in male arteriovenous fistulas. Nature Communications. 2024; 15: 3743. https://doi.org/10.1038/s41467-024-48019-4

[38] Qu Z, Lu Y, Ran Y, Xu D, Guo Z, Cheng M. Chitinase-3 like-protein-1: A potential predictor of cardiovascular disease (Review). Molecular Medicine Reports. 2024; 30: 176. https://doi.org/10.3892/mmr.2024.13300

[39] Liu D, Hu X, Ding X, Li M, Ding L. Inflammatory Effects and Regulatory Mechanisms of Chitinase-3-like-1 in Multiple Human Body Systems: A Comprehensive Review. International Journal of Molecular Sciences. 2024; 25: 13437. https://doi.org/10.3390/ijms252413437

[40] Liang L, Chen Q, Cao W, Tang L, Wei Y, Ding N, et al. Chitinase-3-like protein 1 is an independent risk factor for the early failure of forearm autologous arteriovenous fistulas in uremic patients. Therapeutic Apheresis and Dialysis : Official Peer-reviewed Journal of the International Society for Apheresis, the Japanese Society for Apheresis, the Japanese Society for Dialysis Therapy. 2021; 25: 939–946. https://doi.org/10.1111/1744-9987.13623

[41] Lambert J, Jørgensen HF. Vascular smooth muscle cell phenotypic switching and plaque stability: a role for CHI3L1. Cardiovascular Research. 2021; 117: 2691–2693. https://doi.org/10.1093/cvr/cvab099

[42] Cao G, Xuan X, Hu J, Zhang R, Jin H, Dong H. How vascular smooth muscle cell phenotype switching contributes to vascular disease. Cell Communication and Signaling : CCS. 2022; 20: 180. https://doi.org/10.1186/s12964-022-00993-2

[43] Wang G, Luo Y, Gao X, Liang Y, Yang F, Wu J, et al. MicroRNA regulation of phenotypic transformations in vascular smooth muscle: relevance to vascular remodeling. Cellular and Molecular Life Sciences : CMLS. 2023; 80: 144. https://doi.org/10.1007/s00018-023-04793-w

[44] Mushtaq U, Seh BA, Khanday FA, Ahmad M. CHI3L1: An Emerging Player in Neuroinflammation and Neurodegeneration. Molecular Neurobiology. 2026; 63: 23. https://doi.org/10.1007/s12035-026-05724-z. Erratum in: Molecular Neurobiology. 2026; 63: 443. https://doi.org/10.1007/s12035-026-05724-z

[45] Kumari S, Dhapola R, Reddy DH. Apoptosis in Alzheimer's disease: insight into the signaling pathways and therapeutic avenues. Apoptosis : an International Journal on Programmed Cell Death. 2023; 28: 943–957. https://doi.org/10.1007/s10495-023-01848-y

[46] Lee EH, Kim HT, Chun SY, Chung JW, Choi SH, Lee JN, et al. Role of the JNK Pathway in Bladder Cancer. OncoTargets and Therapy. 2022; 15: 963–971. https://doi.org/10.2147/OTT.S374908

[47] Zhou Y, Yuan Y, Yao X, Wang L, Yao L, Tang D, et al. miPEP31 alleviates sepsis development by regulating Chi3l1-dependent macrophage polarization. Biology Direct. 2024; 19: 117. https://doi.org/10.1186/s13062-024-00568-w

[48] Wang X, Han X, Yu J, Hu F, Huang C, Chen C, et al. Chitinase 3-Like 1 Promotes Endothelial-to-Mesenchymal Transition in Systemic Sclerosis via Mechanistic Target of Rapamycin Complex 1 Signaling Pathway. Arthritis & Rheumatology (Hoboken, N.J.). 2026; 78: 403–417. https://doi.org/10.1002/art.43356

[49] Begum R, Thota S, Abdulkadir A, Kaur G, Bagam P, Batra S. NADPH oxidase family proteins: signaling dynamics to disease management. Cellular & Molecular Immunology. 2022; 19: 660–686. https://doi.org/10.1038/s41423-022-00858-1

[50] Chou HH, Teng MS, Juang JMJ, Chiang FT, Tzeng IS, Wu S, et al. Circulating YKL-40 levels but not CHI3L1 or TRIB1 gene variants predict long-term outcomes in patients with angiographically confirmed multivessel coronary artery disease. Scientific Reports. 2024; 14: 29416. https://doi.org/10.1038/s41598-024-81190-8

[51] Qamar SUR, Spahić L, Benolić L, Zivanovic M, Filipović N. Treatment of Peripheral Artery Disease Using Injectable Biomaterials and Drug-Coated Balloons: Safety and Efficacy Perspective. Pharmaceutics. 2023; 15: 1813. https://doi.org/10.3390/pharmaceutics15071813